Inorganic Chemistry
Article
pubs.acs.org/IC

Understanding the Solution Behavior of Minor Actinides in the Presence of $EDTA^{4-}$, Carbonate, and Hydroxide Ligands

Tamara L. Griffiths,*[†] Leigh R. Martin,[‡] Peter R. Zalupski,[‡] John Rawcliffe,[§] Mark J. Sarsfield,[§] Nick D. M. Evans,[∥] and Clint A. Sharrad*[†,⊥,#]

[†]Centre for Radiochemistry Research, School of Chemistry, The University of Manchester, Oxford Road, Manchester, M13 9PL, U.K.

[‡]Aqueous Separations and Radiochemistry Department, Idaho National Laboratory, P.O. Box 1625, Idaho Falls, Idaho 83415-6150, United States

[§]National Nuclear Laboratory, Sellafield, Seascale, Cumbria, CA20 1PG, U.K.

[∥]Department of Chemistry, Loughborough University, Loughborough, Leicestershire, LE11 3TU, U.K.

[⊥]School of Chemical Engineering and Analytical Science, The University of Manchester, Oxford Road, Manchester, M13 9PL, U.K.;

[#]Research Centre for Radwaste and Decommissioning, Dalton Nuclear Institute, The University of Manchester, Oxford Road, Manchester, M13 9PL, U.K.

Ⓢ *Supporting Information*

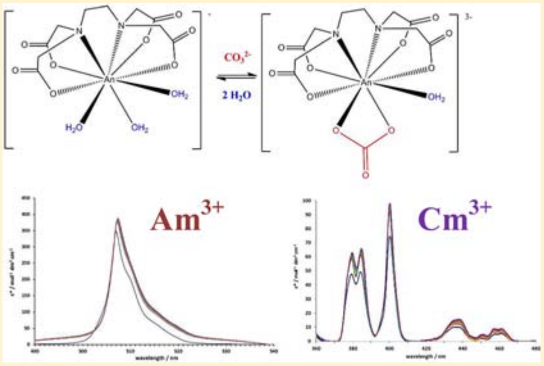

ABSTRACT: The aqueous solution behavior of An^{III} (An = Am or Cm) in the presence of $EDTA^{4-}$ (ethylenediamine tetraacetate), CO_3^{2-} (carbonate), and OH^- (hydroxide) ligands has been probed in aqueous nitrate solution (various concentrations) at room temperature by UV−vis absorption and luminescence spectroscopies (Cm systems analyzed using UV−vis only). Ternary complexes have been shown to exist, including $[An(EDTA)(CO_3)]^{3-}{}_{(aq)}$, (where An = Am^{III} or Cm^{III}), which form over the pH range 8 to 11. It is likely that carbonate anions and water molecules are in dynamic exchange for complexation to the $[An(EDTA)]^-{}_{(aq)}$ species. The carbonate ion is expected to bind as a bidentate ligand and replaces two coordinated water molecules in the $[An(EDTA)]^-{}_{(aq)}$ complex. In a 1:1 $Am^{III}/EDTA^{4-}$ binary system, luminescence spectroscopy shows that the number of coordinated water molecules (N_{H_2O}) decreases from ~8 to ~3 as pH is increased from approximately 1 to 10. This is likely to represent the formation of the $[Am(EDTA)(H_2O)_3]^-$ species as pH is raised. For a 1:1:1 $Am^{III}/EDTA^{4-}/CO_3^{2-}$ ternary system, the N_{H_2O} to the $[Am(EDTA)]^-{}_{(aq)}$ species over the pH range 8 to 11 falls between 2 and 3 (cf. ~3 to ~4 in the binary system) indicating formation of the $[An(EDTA)(CO_3)]^{3-}{}_{(aq)}$ species. As pH is further increased from approximately 10 to 12 in both systems, there is a sharp decrease in N_{H_2O} from ~3 to ~2 in the binary system and from ~2 to ~1 in the ternary system. This is likely to correlate to the formation of hydrolyzed species (e.g., $[Am(EDTA)(OH)]^{2-}{}_{(aq)}$ and/or $Am(OH)_{3(s)}$).

■ INTRODUCTION

The complexation of actinide ions with aminocarboxylate ligands has received much interest over the years because of their relevance in both nuclear reprocessing and geological repositories.[1−5] Ethylenediamine tetraacetate ($EDTA^{4-}$, Figure 1) has been used as a decontaminating agent in the nuclear industry, in defense production of plutonium (Pu), and to treat actinide containing nuclear wastes.[5,6] Currently, there are 1500 tons of radioactive waste containing the $EDTA^{4-}$ ligand.[5]

The $EDTA^{4-}$ ligand is a polyaminocarboxylate, containing hard (4 oxygen) and, in comparison, relatively soft (2 nitrogen) donor groups.[1] $EDTA^{4-}$ provides a hexadentate ligand environment and forms complexes with relatively high thermodynamic stabilities with most metal ions including Am^{III} and Cm^{III} ($\log \beta_{[Am(EDTA)]^-} = 16.4$ and $\log \beta_{[Cm(EDTA)]^-} = 16.7$, both determined in 0.5 M Na^+ electrolyte at 25 °C).[5,7]

Any remaining metal ion coordination sites in the $EDTA^{4-}$-containing complex are typically occupied by water molecules in aqueous solutions or by other ligands that are present in solution.[8] The strong binding affinity of $EDTA^{4-}$ to the trivalent actinides may aid the release and migration of actinides from geological waste repositories into the environment.[5]

Carbonate is an environmentally important and ubiquitous ligand being found in ground and surface waters at concentrations between 10^{-2} and 10^{-5} M.[9] The carbonate ion forms strong ionic interactions, due to its bidentate oxygen donors, with cations of the *f*-elements.[9] These carbonate salts of the 4*f* and 5*f* trivalent ions are generally insoluble over neutral to alkaline pH values, with solubilities less than 10^{-8} M.[10,11]

Received: October 15, 2012
Published: March 15, 2013

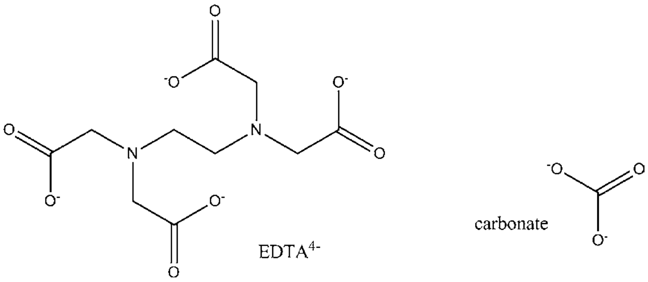

Figure 1. Structures of the $EDTA^{4-}$ and carbonate ligands.

Therefore, the precipitation of trivalent actinide carbonate complexes would prevent the migration of actinides within the environment.

Secondary ligands are able to bind to aquated *f*-ion complexes of $EDTA^{4-}$ by displacing some of the inner sphere water molecules and result in the formation of a ternary complex. This has been shown to occur for selected actinide (Pu^{III}, Am^{III}, and Cm^{III}) and lanthanide (Eu^{III}) complexes of $EDTA^{4-}$ where the secondary complexant is a small organic ligand for example nitrilotriacetate (NTA), iminodiacetate (IDA), oxidiacetate (ODA), and citrate (Figure 1 and the Supporting Information).[8,12−15] Currently, studies that have observed the formation of ternary complexes of the transuranic actinides with small inorganic ligands, such as carbonate, are relatively limited.[16,17] In 1980, Dumonceau et al. reported the discovery of $[Ln(EDTA)(CO_3)]^{3-}_{(aq)}$ (Ln = Nd, Ho, and Er) species in alkaline solution, which were identified spectrophotometrically.[17] The UV−vis absorption spectra, recorded by Dumonceau et al. for the titration of $Na_2CO_{3(aq)}$ into a solution containing $[Ho(EDTA)]^{-}_{(aq)}$, show the presence of two isosbestic points at 448 and 454 nm indicating the formation of the $[Ho(EDTA)(CO_3)]^{3-}_{(aq)}$ complex. The authors also derive stability constants for the formation of the ternary complexes from the measured UV−vis absorption spectra ($\log \beta_{[Nd(EDTA)(CO_3)]^{3-}} = 17.46 \pm 0.12$; $\log \beta_{[Ho(EDTA)(CO_3)]^{3-}} = 19.23 \pm 0.08$ and $\log \beta_{[Er(EDTA)(CO_3)]^{3-}} = 19.61 \pm 0.11$; $I = 2.5$ M $NaNO_3$).[17] More recently in 2003, Boukhalfa et al. reported the formation of a Pu^{IV}−$EDTA^{4-}$−carbonate mixed ligand complex, using potentiometry, at near-neutral pH ($\log \beta_{[Pu(EDTA)(CO_3)]^{2-}} = 35.51 \pm 0.15$; $I = 0.1$ M $NaNO_3$).[16]

We report our studies of the aqueous behavior of Am^{III}−$EDTA^{4-}$ species in the presence and absence of carbonate ions using both UV−vis absorption and luminescence spectroscopies to probe the possibility of ternary complex formation. The use of Am^{III} luminescence to probe complexation behavior and solution speciation is relatively limited, when compared to equivalent Cm^{III} studies.[18−20] This is because Am^{III} has a lower luminescence intensity and shorter luminescence lifetime than Cm^{III}; however, the emissive bands of the Am^{III} ion are still sufficiently intense to obtain reliable information about the coordination environment of the Am^{III} ion.[18,21] Additionally, there are few reports on analyzing alkaline samples using luminescence spectroscopy to probe any metal species, as most reported work details luminescence relevant to the pH of biological systems.[22] We also report the analogous Cm^{III}−$EDTA^{4-}$−carbonate species, which have been investigated using UV−vis absorption spectroscopy.

EXPERIMENTAL SECTION

Radionuclide Warning. ^{243}Am and ^{248}Cm are radionuclides with high specific activities that should only be manipulated in a specifically designated facility in accordance with appropriate safety controls. All spectroscopic measurements were undertaken either in controlled facilities and/or using multiple containment procedures.

$^{243}Am^{III}$ and $^{248}Cm^{III}$ studies were performed at Idaho National Laboratory (INL) and stock radionuclide solutions were obtained in nitric acid solution. The concentrations of Am^{III} and Cm^{III} ions in the stock solutions used at INL were determined by ICP-MS. The initial ionic strength of all working solutions at INL was 0.5 M $NaNO_3$.

$^{243}Am^{III}$ luminescence studies were conducted at National Nuclear Laboratory (NNL), Sellafield, Cumbria, and the Am^{III} stock solution was received in a hydrochloric acid medium. This Am^{III} in aqueous HCl solution was evaporated to dryness under a heat lamp, and then redissolved in a mixed aqueous nitric acid (1.5 M)/sodium nitrate (0.5 M) solution giving a total nitrate concentration of 2 M. Gamma spectroscopy was used to determine the ^{243}Am concentration in samples prepared at NNL. The ^{243}Am energy used was 74.7 keV (with emission probability 67%).

All chemicals were reagent grade or higher. Milli-Q water (18 MΩ) was used in preparations of all solutions. Stock solutions of disodium ethylenediamine tetraacetic acid (Aldrich) and sodium bicarbonate (Aldrich) were prepared by dissolution in water.

UV−vis absorption spectra of solutions containing $^{243}Am^{III}$ and $^{248}Cm^{III}$ were recorded at INL using a Varian Cary-6000i spectrophotometer coupled with a liquid waveguide capillary cell (LWCC) equipped with a fiber optic interface. The cell had an internal volume of 2 mL, a 1 m path length and an effective wavelength range of approximately 300−850 nm. Spectra were recorded between 490 and 540 nm and 350−650 nm for Am^{III} and Cm^{III} containing solutions respectively at 0.1 nm intervals. The initial concentrations of the $[Am(EDTA)]^{-}_{(aq)}$ and $[Cm(EDTA)]^{-}_{(aq)}$ complexes were 5×10^{-5} M and 2×10^{-5} M, respectively. In each titration, appropriate aliquots of the titrant (NaOH or $NaHCO_3$) were added into the cell and mixed thoroughly before each spectrum was collected. A set of 10 to 12 spectra were generated for each UV−vis spectroscopic titration. The electromotive force (EMF, in millivolts) was measured with a Metrohm pH meter (Model 713) equipped with a Ross combination pH electrode (Orion Model 8102) after each titrant addition. The electrode filling solution was 5.0 M $NaCl_{(aq)}$. The linear fit from the electrode calibration was used to calculate the pH from the EMF in the metal−ligand titrations.

Luminescence spectroscopic titrations of $^{243}Am^{III}$ containing solutions were conducted at NNL. A Quantel Brilliant B Nd:YAG laser, which gave an output of 1064 nm, was used to optically pump the tunable dye laser (Quantel TDL-90) after passing through a second harmonic generator (output 532 nm) and third harmonic generator (355 nm). The dye laser was tuned to produce the desired excitation wavelength of 503 nm for Am^{III}. Fiber optics were used to focus the emitted light onto a Acton SpectraPro 2500i spectrograph combined with Princeton instruments, ST-133 controller and Pi-Max Charged Coupled Device (CCD) camera (0.500 m Imaging Triple Grating Monochromator). Data were collected within a gate width of 70 to 120 ns, with a 5.55 ns delay width. The instrument was controlled remotely using *Winspec* software. Data were processed using *Grams/AI* software and analyzed by linear regression on *Microsoft Excel 2007*. A daily mercury/argon (HgAr) wavelength calibration was performed before Am^{III} measurements were recorded. For maximum power output of the laser, the Coumarin 500 dye had to be changed weekly. The Am^{III} containing samples were introduced into the luminescence cuvette using a flow system. The initial concentration of the $[Am(EDTA)]^{-}_{(aq)}$ complex was 4×10^{-4} M. A pH electrode (Cole Palmer Model PC1R2A), calibrated using pH 4, 7, and 11 buffers, was also fitted into the flow circuit to allow pH measurements to be taken. In the luminescence spectroscopy titrations, appropriate aliquots of the titrant (0.1 M NaOH) were added into the cell and mixed thoroughly before each spectrum was collected.

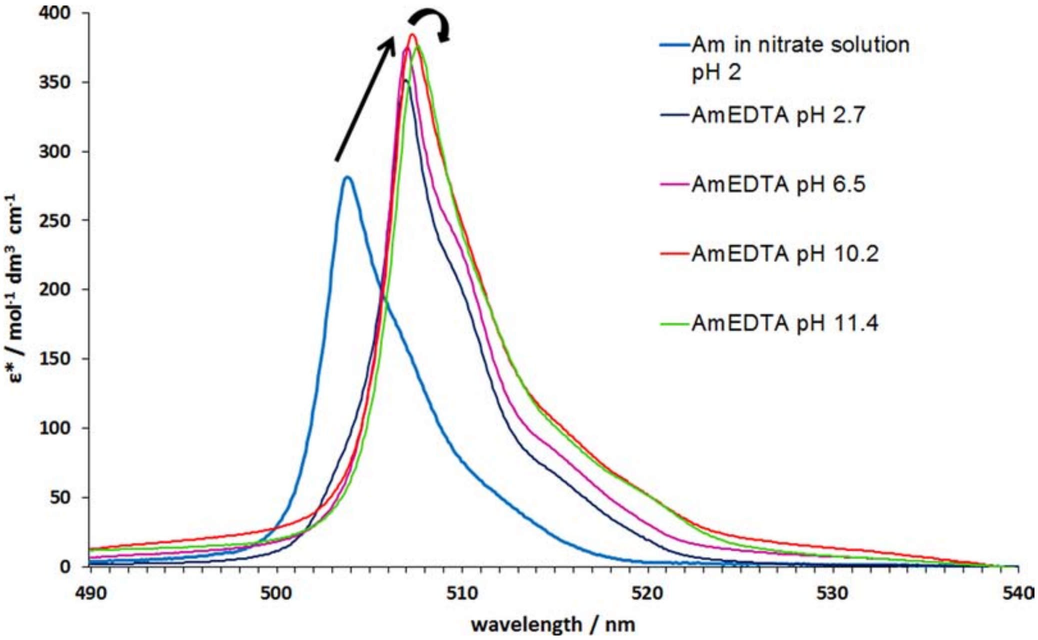

Figure 2. UV−vis absorption spectra for the effect of pH on a 1:1 $Am^{III}/EDTA^{4-}$ system; $[Am^{III}]_i = [EDTA^{4-}]_i = 5 \times 10^{-5}$ M; pH adjusted using 0.01 and 0.1 M NaOH; $I_o = 0.5$ M $NaNO_3$.

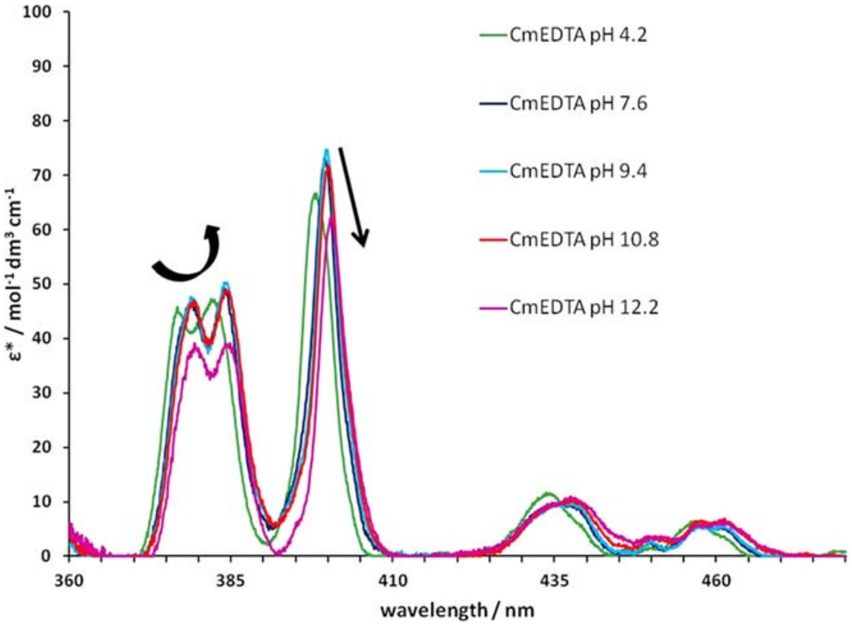

Figure 3. Adjusted UV−vis absorption spectra for the effect of pH on a 1:1 $Cm^{III}/EDTA^{4-}$ system; $[Cm^{III}]_i = [EDTA^{4-}]_i = 2 \times 10^{-5}$ M; pH adjusted using 0.01 and 0.1 M NaOH; $I_o = 0.5$ M $NaNO_3$.

The detector for gamma spectroscopy analysis used was a DSG HPGe photon detector, Model GC10, connected to an Ortec DSPEC jr. digital gamma ray spectrometer operated using *Ortec GammaVision-32* software Version 6. The detectors were calibrated for energy, fwhm (resolution), and efficiency using a mixed gamma nuclide reference standard (QCY48 supplied by HTSL and traceable to national standards).

■ RESULTS AND DISCUSSION

UV−vis Absorption Spectroscopy. *Am^{III}/Cm^{III} −$EDTA^{4-}$ Binary Systems.* Use of a 1 m Liquid Waveguide Capillary Cell (LWCC) allowed for ultrasensitive UV−vis absorbance measurements to be performed and provided a 100 fold enhancement of the signal, compared to a standard 1 cm cuvette. This enabled the analysis of low volumes of solutions containing low concentrations of Am^{III} or Cm^{III} (~10^{-5} M) thus helping to reduce the radiotoxicity of samples being analyzed. Typical optical absorption values for the Am^{III} and Cm^{III} systems at these low concentrations were approximately 2 and 0.5 au respectively and the typical error in all of the presented absorption maxima (λ_{max}) is ±0.1 nm.

The complexation of Am^{III} and Cm^{III} with $EDTA^{4-}$ as a function of pH has been studied by UV−vis absorption spectroscopy (Figures 2 and 3, respectively). The λ_{max} of Am^{III} in aqueous 0.5 M $NaNO_3$ solution is found at 503.9 nm, which corresponds to an electronic transition from the $^7F_0$ ground

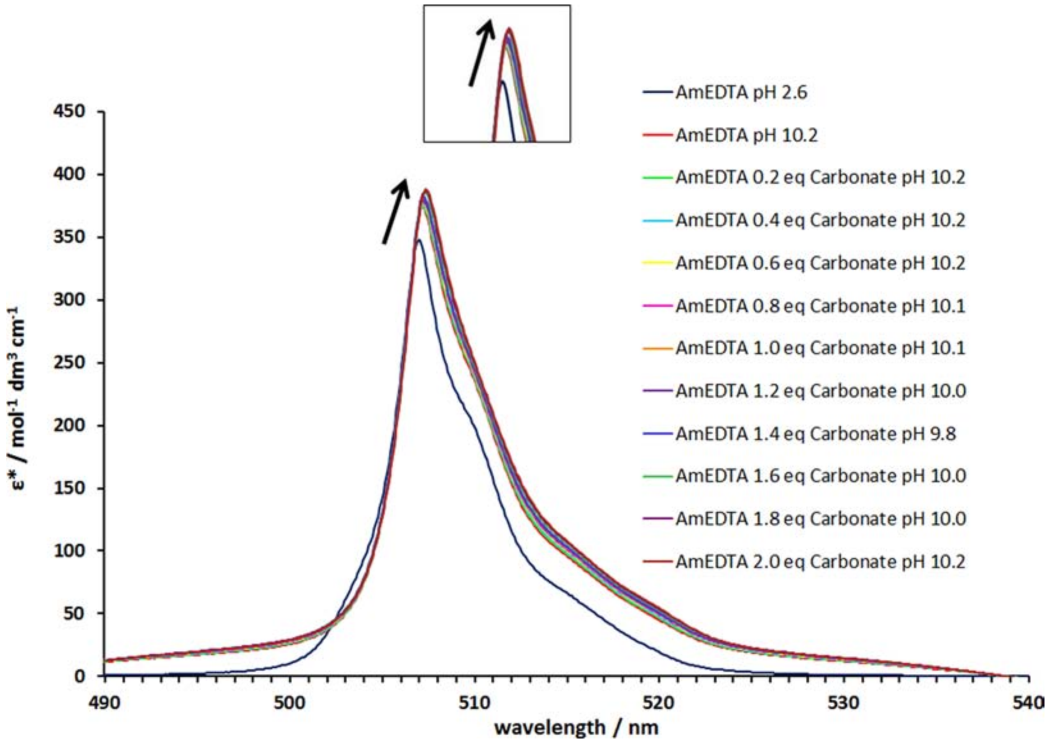

Figure 4. UV−vis absorption spectra for a 1:1:X $\mathrm{Am^{III}/EDTA^{4-}/CO_3^{2-}}$ system (where X = 0 to 2 equivs); $[\mathrm{Am^{III}}]_i = [\mathrm{EDTA^{4-}}]_i = 5 \times 10^{-5}$ M; pH 10 ± 0.5 (adjusted using 0.01 M NaOH or 0.01 M $\mathrm{HNO_3}$); I_o = 0.5 M $\mathrm{NaNO_3}$. Insert: Zoom-in of absorption maxima.

state to the $^5\mathrm{L}_6$ excited state.[23,24] On complexation with $\mathrm{EDTA^{4-}}$, there is a bathochromic shift of the $\lambda_{\max}$ for this transition to 507.0 nm accompanied by an increase in the apparent extinction coefficient (ε*, + 70 $\mathrm{mol^{-1}\ dm^3\ cm^{-1}}$). As the pH of this system is increased from 3 to 11, a very small red-shift (0.7 nm) of the peak maximum occurs coupled with a broadening of the absorption profile. The results are similar to those found in the work reported by Morgenstern et al.,[23] who analyzed an $\mathrm{Am^{III}}$−humate system using UV−vis absorption spectroscopy. They discuss how the bathochromic shift of $\lambda_{\max}$ from 503.1 nm for the aquated $\mathrm{Am^{III}}$ ion to 505.3 nm when humate is added to give a solution of pH 6 corresponds to the formation of an $\mathrm{Am^{III}}$−humate complex.[23] They also detail a shift in $\lambda_{\max}$ from 505.3 to 507.1 nm, a decrease in the molar absorptivity, and a broadening of the absorption band as pH is increased from pH 6.0 to 10.7.[23] They assign these small spectral differences as due to increased formation of an $\mathrm{Am^{III}}$−humate complex and also to the interaction of hydroxide with this complex (i.e., formation of $\mathrm{Am^{III}}$−humate−hydroxide species).[23] In our $\mathrm{Am^{III}}$−$\mathrm{EDTA^{4-}}$ system, the small red-shift in $\lambda_{\max}$ as the pH is raised from 3 to 9 is most likely due to an increase in the formation of the $[\mathrm{Am(EDTA)}]^-_{(aq)}$ complex. There may also be some deprotonation of the bound EDTA ligand over the pH region 2 to 7. This would cause a change in the average denticity of the EDTA ligand to the $\mathrm{Am^{III}}$ cation (i.e., conversion from $[\mathrm{Am(EDTAH)}]_{(aq)}$ to $[\mathrm{Am(EDTA)}]^-_{(aq)}$). This has been previously observed in $\mathrm{La^{III}}$−$\mathrm{EDTA^{4-}}$ containing systems, where the $[\mathrm{La(EDTAH)}]_{(aq)}$ species is dominant from pH 2 to 4. As pH is increased further in this system, the $[\mathrm{La(EDTAH)}]_{(aq)}$ species deprotonates to form the $[\mathrm{La(EDTA)}]^-_{(aq)}$ complex (Supporting Information for the speciation diagram).[7] At pH values greater than 11, the apparent extinction coefficient of the $\mathrm{Am^{III}}$−$\mathrm{EDTA^{4-}}$ system begins to decrease (−8 $\mathrm{mol^{-1}\ dm^3\ cm^{-1}}$), which may be due to the formation of hydrolyzed species (e.g., $[\mathrm{Am(EDTA)(OH)}]^{2-}_{(aq)}$ and $\mathrm{Am(OH)_{3(s)}}$) as also observed by Morgenstern et al.[23] The precipitation of $\mathrm{Am(OH)_{3(s)}}$ was not directly observed in the experiments possibly because low metal ion concentrations were used (i.e., ≤ 5×10^{-5} M). However, the precipitation of small amounts of $\mathrm{An(OH)_{3(s)}}$ (An = $\mathrm{Am^{III}}$ or $\mathrm{Cm^{III}}$) must be considered possible at high pH in all of the systems studied. In the 1:1 $\mathrm{An^{III}/EDTA^{4-}}$ binary systems, $\mathrm{CO_2}$ was not excluded from the system. Precipitates such as $\mathrm{Am(CO_3)(OH)_{(s)}}$ have been reported to form in $\mathrm{CO_2}$ saturated solutions and under varying partial pressures of $\mathrm{CO_2}$;[25] however, it is unlikely that this precipitate would form under the conditions used in our study. The lack of observation of $\mathrm{An(OH)_3}$ or $\mathrm{An_2(CO_3)_3}$ precipitates in this study, under alkaline conditions, further illustrates the strong binding affinity of $\mathrm{EDTA^{4-}}$ to the trivalent actinides. It is expected that polyaminocarboxylic ligands, such as $\mathrm{EDTA^{4-}}$, are able to increase the solubility of actinide metal ions, which may have implications in aiding the release and migration of actinides from geological waste repositories into the environment.

All of the measured UV−vis spectra of the $\mathrm{Cm^{III}}$ solutions studied display sharp and relatively weak absorption bands, as expected for f−f transitions, upon an intense, broad transition in the UV region of the spectrum (Supporting Information). This broad absorption has been previously observed in the spectra of $\mathrm{Cm^{III}}$ solutions, and has been attributed to radiolytic decomposition of water with time.[26] All $\mathrm{Cm^{III}}$ spectra presented have been adjusted by fitting and subtracting the broad transition in the UV region to distinguish between changes in the $\mathrm{Cm^{III}}$ absorption profile and solvent decomposition.

The UV−vis spectrum of 1:1 $\mathrm{Cm^{III}/EDTA^{4-}}$ at pH 4.2 shows absorption bands at 377, 382, 398, 434, and 456 nm (Figure 3), of which the most intense band at 398 nm

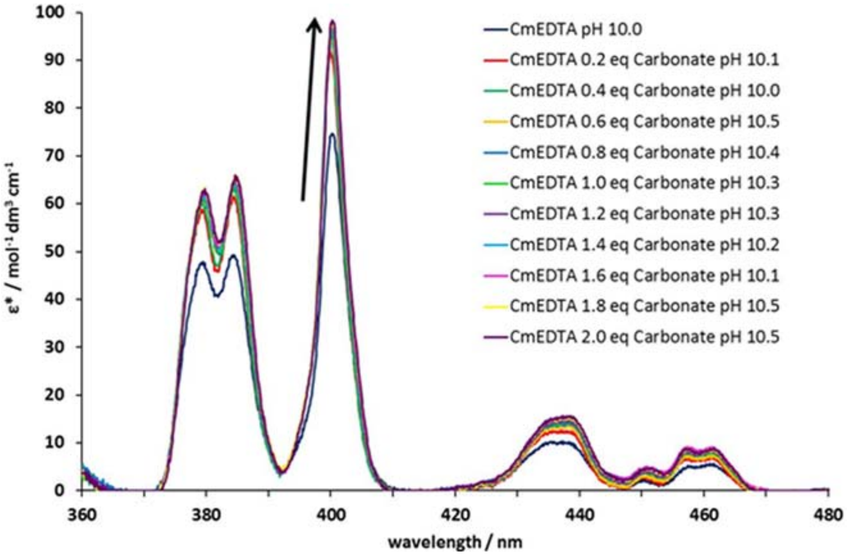

Figure 5. Adjusted UV−vis absorption spectra for a 1:1:X $Cm^{III}/EDTA^{4-}/CO_3^{2-}$ system (where X = 0 to 2 equivalents); $[Cm^{III}]_i = [EDTA^{4-}]_i = 2 \times 10^{-5}$ M; pH 10 ± 0.5 (adjusted using 0.01 M NaOH or 0.01 M HNO_3); I_o = 0.5 M $NaNO_3$.

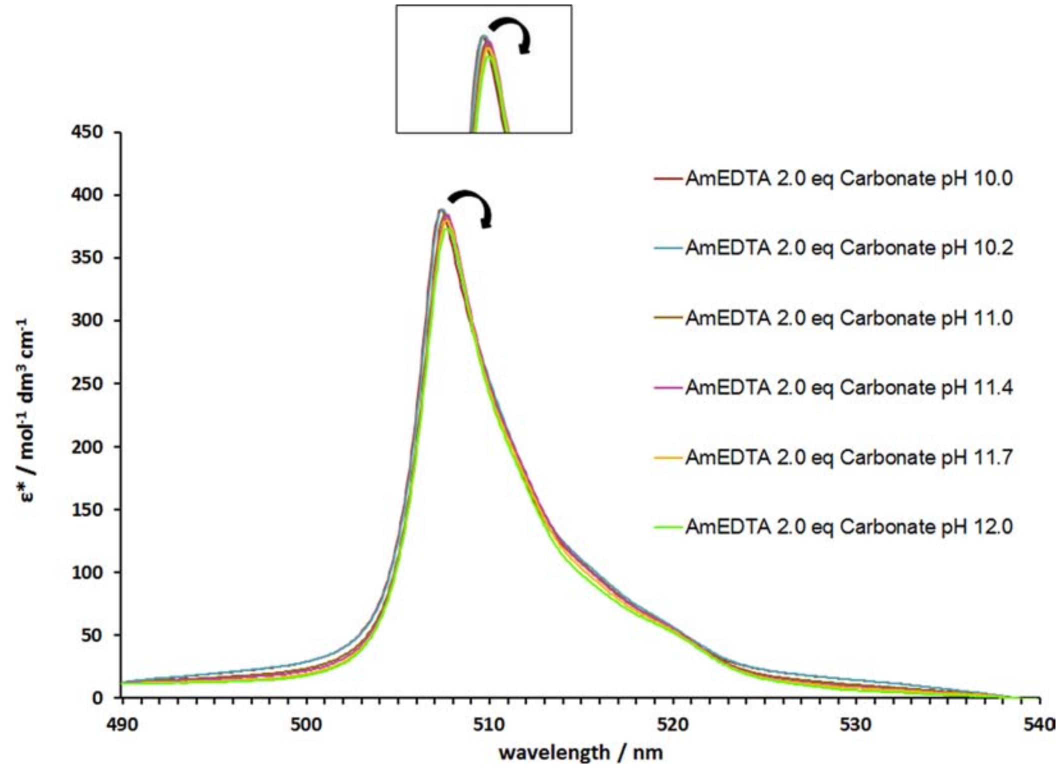

Figure 6. UV−vis absorption spectra for the effect of pH on a 1:1:2 $Am^{III}/EDTA^{4-}/CO_3^{2-}$ system; $[Am^{III}]_i = [EDTA^{4-}]_i = 5 \times 10^{-5}$ M; $[CO_3^{2-}]_i = 1 \times 10^{-4}$ M; titrated with 0.1 M NaOH; I_o = 0.5 M $NaNO_3$. Insert: Zoom-in of absorption maxima.

corresponds to the electronic transition from the $^8S_{7/2}$ ground state to the $^6I_{17/2}$ excited state.[4,5] Raising the pH of the 1:1 $Cm^{III}/EDTA^{4-}$ system from pH 4.2 to 10.8 causes a red shift in all of the transitions (+2.1 nm for the λ_{max} at 397.9 nm), coupled with an increase in the apparent extinction coefficient (+5 mol^{-1} dm^3 cm^{-1} for the λ_{max} at 397.9 nm) of the Cm^{III} absorption profile. This is likely to represent an increase in the formation of the $[Cm(EDTA)]^-_{(aq)}$ complex, similar to the analogous Am^{III} system. Above pH 10.8, the observed decrease in the apparent extinction coefficients (−9 mol^{-1} dm^3 cm^{-1}) of the transitions in the Cm^{III} spectra indicates a change in speciation, which is likely to be due to the formation of Cm^{III} containing hydrolyzed species (e.g., $[Cm(EDTA)(OH)]^{2-}_{(aq)}$ or $Cm(OH)_{3(s)}$).

An^{III}−$EDTA^{4-}$ −Carbonate Ternary Systems. An = Am and Cm. The UV−vis absorption spectra of a 1:1 $An^{III}/EDTA^{4-}$ system (where An = Am or Cm) have been measured as a function of carbonate ion concentration (Figures 4 and 5, respectively) at pH 10 ± 0.5 adjusted using NaOH or HNO_3. The pH of the 1:1 $An^{III}/EDTA^{4-}$ systems were initially increased to approximately pH 10, using NaOH, before the addition of carbonate ions. As the carbonate ion concentration

is increased in the 1:1 An^{III}/$EDTA^{4-}$ systems, there is a growth in the apparent extinction coefficient [+13 mol^{-1} dm^3 cm^{-1} and +24 mol^{-1} dm^3 cm^{-1} for Am^{III} (λ_{max} = 507.3 nm) and Cm^{III} (λ_{max} = 400.2 nm), respectively] and a slight red shift of the absorption maxima (+0.3 nm for both Am^{III} and Cm^{III}). The growth in the apparent extinction coefficient and slight red shift of the absorption maxima, coupled with no evidence for the precipitation of $An_2(CO_3)_3$ (likely solubility-controlling precipitate)[25] in the presence of $EDTA^{4-}$, indicates the formation of the $[An(EDTA)(CO_3)]^{3-}{}_{(aq)}$ species. The analogous complexes for Pu^{IV} and Ln^{III} have been previously shown to form in similar solution conditions providing further credibility to the argument that these subtle changes in the spectral profiles are due to the formation of minor actinide ternary complexes.[16,17] The apparent extinction coefficient in the 1:1:*X* An^{III}/$EDTA^{4-}$/$CO_3{}^{2-}$ system (where *X* = 0 to 2) continues to increase up to two equivalents of carbonate ions. These small spectral changes are likely to reflect the position of the equilibrium being favored toward the formation of the $[An(EDTA)(CO_3)]^{3-}{}_{(aq)}$ species. It is unlikely that the $[An(EDTA)(CO_3)_2]^{5-}{}_{(aq)}$ species is formed, which is discussed below (luminescence spectroscopy section on the Am^{III}–$EDTA^{4-}$ –carbonate ternary system).

The effects of pH, adjusted using NaOH, on the absorption spectra of the 1:1:2 Am^{III}/$EDTA^{4-}$/$CO_3{}^{2-}$ system are shown in Figure 6. As pH is increased from 10 to 12, the apparent extinction coefficient decreases (−16 mol^{-1} dm^3 cm^{-1}), and a slight red-shift of the peak maximum (+0.3 nm) occurs after pH 11. It may be possible that these observations are due to the carbonate anion being replaced by the hydroxide ion/s above pH 11, which is consistent with previously mentioned hydrolysis effects on the absorption profile. It has been reported that hydrolyzed minor actinide species are likely to dominate over minor actinide carbonate complexes at pH values near 11.[25]

Attempts were made to determine the stability constants for the $[An(EDTA)]^{-}{}_{(aq)}$ and $[An(EDTA)(CO_3)]^{3-}{}_{(aq)}$ species (An = Am or Cm) by fitting the spectroscopic titration data to appropriate speciation models using the *Hyperquad* software.[27] Stability constants were refined for these species but had significant errors due to the small number of spectra obtained. Refined log β values for the $[An(EDTA)]^{-}{}_{(aq)}$ complex range between 14 to 16, which is similar to previously obtained stability constants for these species in slightly different solution conditions ($\log \beta_{[Am(EDTA)]^-} = 16.4$ and $\log \beta_{[Cm(EDTA)]^-} = 16.7$, both determined in 0.5 M Na^+ electrolyte at 25 °C).[7] For $[Am(EDTA)]^{-}{}_{(aq)}$, the stability constant information obtained from the UV–vis data is consistent with the speciation behavior observed by luminescence spectroscopy (i.e., $\log \beta < 16.4$; discussed in luminescence section). Refined log *K* values for the binding of carbonate to the $[An(EDTA)]^{-}{}_{(aq)}$ complex are found to be approximately 3 to 4. These are consistent with expected binding constants ($\log K < 5$) of secondary ligands (e.g., citrate, NTA, IDA) to $[M(EDTA)]^{-}{}_{(aq)}$ complexes (where M = Am^{III}, Cm^{III}, Pu^{III}, Eu^{III}).[15]

Time-Resolved Laser Induced Fluorescence Spectroscopy of $^{243}Am^{III}$. Time-resolved laser induced fluorescence spectroscopy (TRLIFS) can be used to study Am^{III} complexation with organic ligands in aqueous solution by determining the number of coordinated water molecules in the first coordination shell of the Am^{III} ion.[28] The time-resolved emission spectra of the $Am^{III}{}_{(aq)}$ ion, upon excitation at 503 nm, show emissions at approximately 691 and 833 nm (Figure 7), which are due to the $^5D_1 \rightarrow {}^7F_1$ and the $^5D_1 \rightarrow {}^7F_2$ transitions, respectively.[29] Typically the emission band at 691 nm is used to probe Am^{III} complexation behavior due to the relatively high emission intensity;[23,18,28,29] therefore, only this band has been analyzed in the work presented here. A plot of the intensity of the signal at λ_{max} versus the gate delay (Supporting Information) illustrates the exponential decay of the signal after each 10 ns delay. A plot of ln(intensity) versus the gate delay (Supporting Information) gives a linear fit, from which the luminescence lifetime (τ) can be calculated using eq 1.

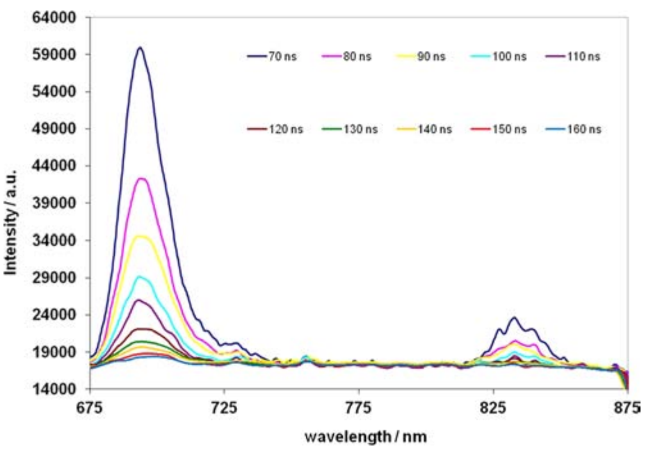

Figure 7. Time-resolved emission spectra of the $Am^{III}{}_{(aq)}$ ion, $[Am^{III}] = 4 \times 10^{-4}$ M, *I* = 0.02 M HNO_3.

$$\tau = -\frac{1}{m} \qquad (1)$$

where: τ = luminescent lifetime (ns); *m* = gradient of ln(intensity) versus the gate delay plot.

The luminescence lifetime of the $Am^{III}{}_{(aq)}$ ion in 0.02 M HNO_3 aqueous solution was calculated to be 24.1 ± 1.2 ns at room temperature (RT). This is in good agreement with previously reported luminescence lifetimes of $Am^{III}{}_{(aq)}$, which range from 22 to 25 ns at 22 to 25 °C in 0.01 to 0.10 M $HClO_4$ solution (pH not specified).[23,28,29]

The luminescence lifetimes can subsequently be used to determine the inner-sphere hydration number of the metal ion (N_{H_2O}), thereby providing information on the metal ion coordination environment in solution.[23] We have used the equation derived by Kimura et al.[30] to calculate the N_{H_2O} coordinated to the Am^{III} ion in various solution conditions from the luminescence lifetimes (eq 2).

$$N_{H_2O} = \left(\frac{2.56 \times 10^{-7}}{\tau}\right) - 1.43 \qquad (2)$$

The value of the N_{H_2O} coordinated to the $Am^{III}{}_{(aq)}$ ion in 0.02 M HNO_3 is calculated to be approximately nine.[30] There are reports that detail nine inner-sphere water molecules associated with the Am^{III} ion in aqueous solutions (pH not specified), characterized using absorption and luminescence spectroscopies, and 10 water molecules coordinated to the $Am^{III}{}_{(aq)}$ ion in dilute aqueous chloride solutions (pH not specified) determined by X-ray absorption fine structure (XAFS) spectroscopy.[31] The structure of the $[Am(H_2O)_9]^{3+}$ species (crystals grown from trifluoromethanesulfonate media, pH not specified) has been reported previously, where the Am^{III} ion coordinates in a tricapped, trigonal prismatic geometry.[31,32] In accordance with the luminescence and absorption spectroscopies performed on aqueous solutions of the Am^{III} ion, as well as the reported structure of the $[Am(H_2O)_9]^{3+}$ species, it is assumed that the $Am^{III}_{(aq)}$ coordination number will be nine for the purposes of this work.

Am^{III}–$EDTA^{4-}$ Binary System. The 1:1 $Am^{III}/EDTA^{4-}$ system in aqueous nitrate solution (2 M) has been examined using luminescence spectroscopy. The initial value of the N_{H_2O} coordinated to the $Am^{III}_{(aq)}$ ion at pH 0.5 in 2 M aqueous nitrate solution is calculated to be 7.6 ± 0.6 (no $EDTA^{4-}_{(aq)}$ present), which may correspond to some formation of the $[Am(NO_3)(H_2O)_7]^{2+}$ species in concentrated aqueous nitrate solutions (as shown in the speciation diagram, Supporting Information). The addition of $EDTA^{4-}_{(aq)}$ to this solution causes the luminescence lifetime to increase and it continues to do so as pH is raised from approximately pH 1 to 12 (Supporting Information). Subsequently, the N_{H2O} bound to the Am^{III} ion in this system decreases (Figure 8). This indicates that as pH is increased, the equilibria between the free $Am^{III}_{(aq)}$ ion and NO_3^- to give the $[Am(NO_3)]^{2+}_{(aq)}$ complex, and the free $Am^{III}_{(aq)}$ ion and the $EDTA^{4-}$ ligand forming the $[Am(EDTA)]^-_{(aq)}$ complex, is favored toward $EDTA^{4-}$ complex formation, as expected. This reduction in N_{H_2O} bound to the Am^{III} ion causes the luminescence lifetime to increase as there are fewer OH oscillators to quench the Am^{III} excited state.[26] At pH 10.5, the N_{H_2O} bound to the Am^{III} ion is calculated to be approximately three, which can be represented by the $[Am(EDTA)(H_2O)_3]^-$ species. At pH 12, the N_{H_2O} bound to the $[Am(EDTA)]^-_{(aq)}$ species reduces to 1.8 ± 0.3, and so hydrolyzed species are likely to be formed (i.e., $[Am(EDTA)(OH)]^{2-}_{(aq)}$ and $Am(OH)_{3(s)}$).

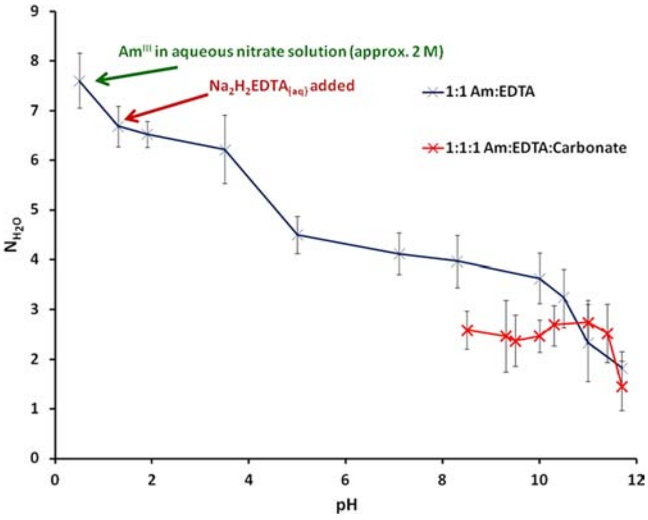

Figure 8. Effect of pH on the N_{H_2O} bound to the Am^{III} ion in the 1:1 $Am^{III}/EDTA^{4-}$ ($[Am^{III}]_i = [EDTA^{4-}]_i = 4 \times 10^{-4}$ M, in approximately 0.5 M $NaNO_3$/1.5 M HNO_3 solution) and 1:1:1 $Am^{III}/EDTA^{4-}/CO_3^{2-}$ systems ($[Am^{III}]_i = [EDTA^{4-}]_i = [CO_3^{2-}]_i = 4 \times 10^{-4}$ M, in approximately 0.5 M $NaNO_3$/1.5 M HNO_3 solution). Solutions titrated using 0.01 and 0.1 M NaOH. Average percentage error bars have been included for all plots of N_{H_2O} vs pH.

Taking the assumption that the only species present in solution between pH 1 to 10 are $[Am(H_2O)_9]^{3+}/[Am(NO_3)(H_2O)_7]^{2+}$ and $[Am(EDTA)(H_2O)_3]^-$, the N_{H_2O} determined by luminescence can be used to assess the speciation of Am^{III} ion in the presence of $EDTA^{4-}$ (and its protonated analogues) with respect to pH (Figure 9). This speciation diagram shows that the percentage formation of the $[Am(EDTA)]^-_{(aq)}$ complex increases from approximately 24% to 85% over the pH range 3.5 to 10.0.

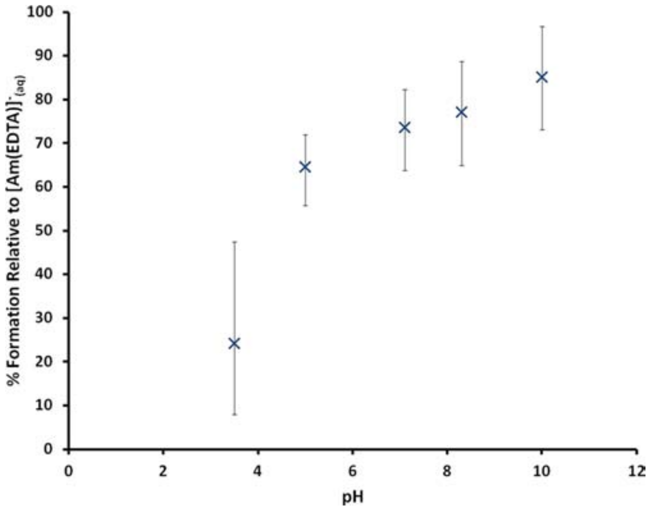

Figure 9. Plot of the percentage formation of the $[Am(EDTA)(H_2O)_3]^-_{(aq)}$ species as a function of pH.

The stability constants for $[Am(EDTA)]^-_{(aq)}$ (log $\beta_{[Am(EDTA)]^-}$ = 16.4 in 0.5 M Na^+ electrolyte at 25 °C), $[Am(NO_3)]^{2+}_{(aq)}$ (log $\beta_{[Am(NO3)]^{2+}}$ = 0.2 in 2 M NH_4ClO_4 electrolyte at 25 °C) and $Am(OH)_{3(s)}$ (log $\beta_{[Am(OH)]^{2+}}$ = 6.4 in 0.7 M NaCl electrolyte at 20 °C) have been previously determined using potentiometry.[7] The speciation diagram for the 1:1 $Am^{III}/EDTA^{4-}$ system, derived from these known equilibrium constants, is displayed in Figure 10.[7] This shows that from pH 0 to 2, the $[Am(NO_3)]^{2+}_{(aq)}$ species dominates the speciation of the Am^{III} ion, while from pH 2 to 11, the $[Am(EDTA)]^-_{(aq)}$ species is dominant. Hydrolysis of the Am^{III} ion to form $[Am(EDTA)(OH)]^{2-}_{(aq)}$ and $Am(OH)_{3(s)}$ is expected to dominate at pH greater than 11.

It is unlikely that there is significant formation of the $[Am(EDTA)(NO_3)]^{2-}_{(aq)}$ species in this system due to the relatively small log β value of $[Am(NO_3)]^{2+}$ (0.2 in 2 M NH_4ClO_4 electrolyte at 25 °C) indicating only relatively weak interactions occur between Am^{III} and NO_3^-.[7] The speciation diagram in Figure 10 indicates that nitrate is in competition with $EDTA^{4-}$ for binding to the Am^{III} ion and, as pH is increased, hydroxide ions will then compete with nitrate for binding to the remaining sites of the Am^{III} ion. For these reasons, we believe that the formation of the $[Am(EDTA)(NO_3)]^{2-}_{(aq)}$ species is negligible.

Differences in the speciation diagrams presented in Figures 9 and 10 suggest that other equilibria may be present at both acidic and alkaline pH. For example, in the acidic pH region, there may be an equilibrium between the $[Am(EDTAH)]_{(aq)}$ and $[Am(EDTA)]^-_{(aq)}$ species (i.e., pentadentate vs hexadentate $EDTA^{4-}$ coordination). Similarly, at alkaline pH, the $[Am(EDTA)]^-_{(aq)}$ complex may be in equilibrium with the hydrolyzed species, $[Am(EDTA)(OH)]^{2-}_{(aq)}$. Therefore, as the formation constants of the $[Am(EDTAH)]_{(aq)}$ and [Am-

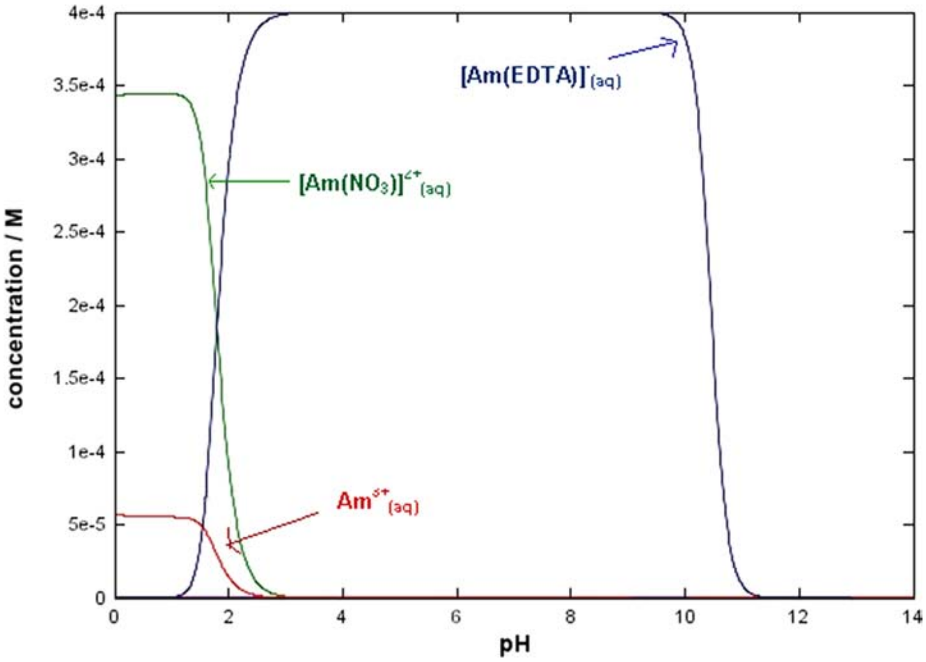

Figure 10. Speciation diagram of a 1:1 $Am^{III}/EDTA^{4-}$ system as a function of pH using the *JCHESS* code.[33] Total [Am^{III}] = total [$EDTA^{4-}$] = 4 × 10^{-4} M, [$NaNO_3$] = 2 M. Only soluble species are shown. Thermodynamic data obtained from the integrated *JCHESS* database, as well as Martell and Smith (corrected to zero ionic strength using the Davies equation).[7].

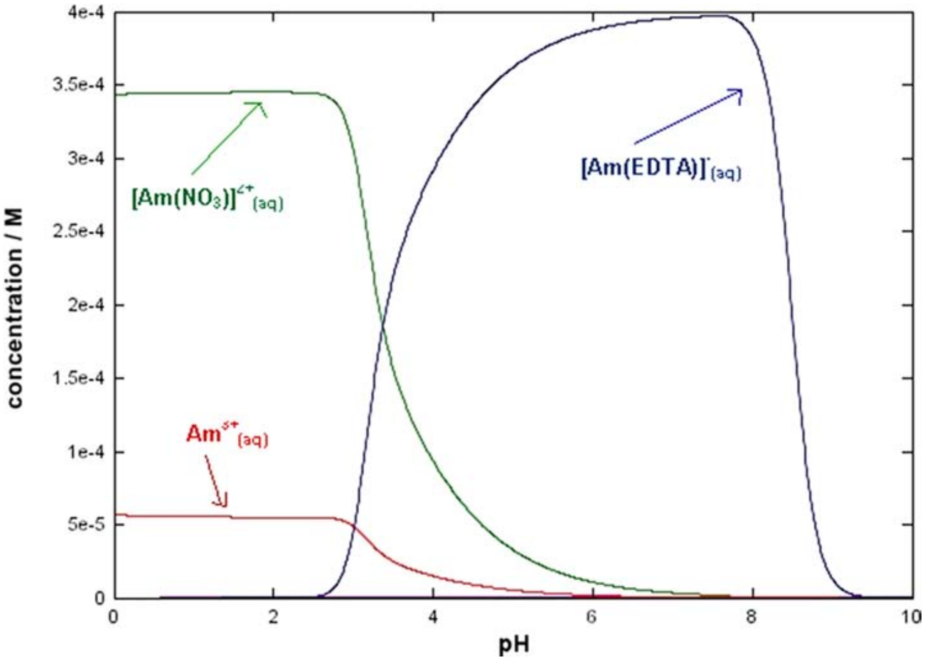

Figure 11. Speciation diagram of a 1:1 $Am^{III}/EDTA^{4-}$ system as a function of pH using the *JCHESS* code with a reduced log $\beta_{[Am(EDTA)]^-}$ value compared to that used in Figure 10.[33] Total [Am^{III}] = total [$EDTA^{4-}$] = 4 × 10^{-4} M; [$NaNO_3$] = 2 M. Only soluble species are shown. Thermodynamic data obtained from the integrated *JCHESS* database, as well as Martell and Smith (corrected to zero ionic strength using the Davies equation).[7].

$(EDTA)(OH)]^{2-}{}_{(aq)}$ species are unknown, discrepancies in the calculated speciation diagram (Figure 10) may occur.

Possible structures of these solution species, which cause the discrepancies between the speciation diagrams derived from potentiometry and luminescence spectroscopy for the 1:1 $Am^{III}/EDTA^{4-}$ system, are displayed in the Supporting Information. Although the equilibria between these species are likely to occur in the pH range studied, the formation of these species will not cause the gradual change of N_{H_2O} from ~8 to ~3 over pH 1 to 10 observed by luminescence spectroscopy.

The differences between the speciation diagrams illustrated in Figures 9 and 10 are most likely due to the established log $\beta_{[Am(EDTA)]^-}$ value of 16.4 (determined in 0.5 M Na^+ electrolyte at 25 °C; note, anion not stated)[7] not being correct for the system that we have used in the luminescence studies (1.5 M HNO_3 and 0.5 M $NaNO_3$ mixed solution at room temperature). A replot of the speciation diagram keeping all other factors the same as shown in Figure 10 but reducing the log $\beta_{[\mathrm{Am(EDTA)}]^-}$ value from 19.6 (established value corrected to zero ionic strength) to 14 (hypothetical value) is presented in Figure 11. The reduced log $\beta_{[\mathrm{Am(EDTA)}]^-}$ value causes a relatively gradual increase in the concentration of the $[\mathrm{Am(EDTA)}]^-{}_{(aq)}$ species as pH is raised from 2.7 to 8, in contrast to the sharp increase in $[\mathrm{Am(EDTA)}]^-{}_{(aq)}$ concentration as pH increases from 1 to 3 when log $\beta_{[\mathrm{Am(EDTA)}]^-}$ value is 19.6 (Figure 10), which gives a reasonable correlation with the speciation profile obtained from our luminescence experiments. Therefore, indicating the log $\beta_{[\mathrm{Am(EDTA)}]^-}$ value in 2 M NO_3^- is lower than what might be expected from previous studies. The predicted speciation profile (Figure 11) shows a decrease in the concentration of the $[\mathrm{Am(EDTA)}]^-{}_{(aq)}$ species above pH 8 due to the formation of insoluble hydrolysis products. However, it is expected that a soluble hydrolyzed species, $[\mathrm{Am(EDTA)(OH)}]^{2-}{}_{(aq)}$, forms above pH 8, but has not been modeled in the speciation diagram.

Am^{III}–$EDTA^{4-}$–Carbonate Ternary System. Luminescence spectroscopy performed on the 1:1:1 $\mathrm{Am^{III}/EDTA^{4-}/CO_3^{2-}}$ system as a function of pH, adjusted using NaOH, shows that the luminescence lifetime of the excited Am^{III} species has increased in the presence of carbonate ions compared to when carbonate ions are absent in the system (Supporting Information). It is likely that the carbonate anion is replacing inner-sphere water molecules in the $[\mathrm{Am(EDTA)}]^-{}_{(aq)}$ complex and so decreasing the number of OH oscillators that quench Am^{III} luminescence. Overlaying the data for the N_{H_2O} bound to the Am^{III} ion in the 1:1 $\mathrm{Am^{III}/EDTA^{4-}}$ and the 1:1:1 $\mathrm{Am^{III}/EDTA^{4-}/CO_3^{2-}}$ systems shows a decrease in the N_{H_2O} coordinated to the $[\mathrm{Am(EDTA)}]^-{}_{(aq)}$ complex from between ~3 and ~4, to between ~2 and ~3, over the pH range 8 to 11 (Figure 8). This is indicative of the carbonate anion either in dynamic exchange with water molecules for coordination to the $[\mathrm{Am(EDTA)}]^-{}_{(aq)}$ complex (Supporting Information), and/or only a fraction of the $[\mathrm{Am(EDTA)}]^-{}_{(aq)}$ complex is converted to the $[\mathrm{Am(EDTA)(CO_3)}]^{3-}{}_{(aq)}$ species under these solution conditions. Above pH 11, the N_{H_2O} coordinated to the $[\mathrm{Am(EDTA)}]^-{}_{(aq)}$ complex decreases to 1.4 ± 0.5. This is likely to correlate to the formation of hydrolyzed species (e.g., $[\mathrm{Am(EDTA)(OH)}]^{2-}{}_{(aq)}$ and/or $\mathrm{Am(OH)_{3(s)}}$).

An excess of carbonate ions added to the 1:1 $\mathrm{Am^{III}/EDTA^{4-}}$ system showed no significant difference in the luminescence lifetime of the $[\mathrm{Am(EDTA)(CO_3)(H_2O)}]^{3-}{}_{(aq)}$ species. Therefore, it is unlikely that two carbonate anions are coordinating to the $[\mathrm{Am(EDTA)}]^-{}_{(aq)}$ complex.

■ CONCLUSIONS

We have provided a deeper qualitative insight into the nature of minor actinide coordination chemistry in mixed-ligand environments over a wide pH range. The formation of An-organic and mixed $[\mathrm{An(organic)(inorganic)}]^{n-}{}_{(aq)}$ complexes (i.e., An = Am or Cm, organic = $EDTA^{4-}$, and inorganic = OH^- or CO_3^{2-}) increase the solubility of minor actinide ions at high pH.

In $\mathrm{An^{III}/EDTA^{4-}/CO_3^{2-}}$ ternary systems, the interaction of CO_3^{2-} with $[\mathrm{An(EDTA)}]^-{}_{(aq)}$ complexes was predominantly observed over the pH range 8 to 11. Use of luminescence spectroscopy to calculate the N_{H_2O} bound to the Am^{III} ion in the 1:1 $\mathrm{Am^{III}/EDTA^{4-}}$ and the 1:1:1 $\mathrm{Am^{III}/EDTA^{4-}/CO_3^{2-}}$ systems over the pH range 8 to 11, showed a reduction in N_{H_2O} in the ternary system compared to the binary system. This suggests that equilibria between binary and ternary species exist in solution.

In experiments where $\mathrm{An^{III}/EDTA^{4-}/CO_3^{2-}}$ ternary complexes were shown to exist, it is likely that hydroxide replaces the carbonate when the pH is greater than 10 in preference to replacing the $EDTA^{4-}$. This is due to the greater thermodynamic coordination stability obtained by high denticity ligands (e.g., $EDTA^{4-}$) relative to that generally observed with low denticity ligands (e.g., CO_3^{2-}).

The lack of observation of $\mathrm{An(OH)_3}$ or $\mathrm{An_2(CO_3)_3}$ precipitates in alkaline conditions (up to pH 11) illustrates the strong binding affinity of $EDTA^{4-}$ to the trivalent actinides. It is proposed that polyaminocarboxylic ligands, such as $EDTA^{4-}$, are able to increase the solubility of actinide metal ions, which may have implications of aiding the release and migration of actinides from geological waste repositories into the environment.

At low pH values between 2 to 3, the $[\mathrm{An(EDTAH)}]_{(aq)}$ species may be dominant in the systems studied (cf. $[\mathrm{La(EDTAH)}]_{(aq)}$ species).[12] However, there are no reported log β values for the formation of the $[\mathrm{An(EDTAH)}]_{(aq)}$ species. Further work will investigate methods that will allow the accurate determination of stability constants related to the formation of ternary complexes of the minor actinides and other species found in these studies.

It is envisaged that the determination of metal ion speciation using a combination of UV–vis absorption and luminescence spectroscopies could be applied to new characterization challenges the nuclear industry will encounter in the future.

■ ASSOCIATED CONTENT

Ⓢ Supporting Information

This material is available free of charge via the Internet at http://pubs.acs.org.

■ AUTHOR INFORMATION

Corresponding Author

*E-mail: Clint.A.Sharrad@manchester.ac.uk.

Notes

The authors declare no competing financial interest.

■ ACKNOWLEDGMENTS

This work was supported by the Nuclear Decommissioning Authority U.K. (student bursary for TLG, research fellowship for CAS and the work at NNL), the University of Manchester Alumni Fund (TLG), and also the RCUK Energy Programme through its support of the MBase consortium. The work at INL was supported from the DOE NE FCR&D Thermodynamics and Kinetics program, under DOE Idaho Operations Office Contract DE-AC07-05ID14517. We wish to acknowledge helpful discussions with Louise Natrajan on the luminescence work.

■ REFERENCES

(1) Choppin, G. R.; Thakur, P.; Mathur, J. N. *C. R. Chimie* **2007**, *10*, 916–928.

(2) Hummel, W.; Puigdomènech, I.; Rao, L.; Tochiyama, O. *C. R. Chimie* **2007**, *10*, 948–958.

(3) Lambert, T. N.; Jarvinen, G. D.; Gopalan, A. S. *Tetrahedron Lett.* **1999**, *40*, 1613–1616.

(4) Wood, S. A. *Eng. Geol.* **1993**, *34*, 229–259.

(5) Thakur, P.; Conca, J. L.; Choppin, G. R. *J. Solution Chem.* **2012**, *41*, 599−615.

(6) Rai, D.; Moore, D. A.; Rosso, K. M.; Felmy, A. R.; Bolton, H. *J. Solution Chem.* **2008**, *37*, 957−986.

(7) (a) Smith, R. M.; Martell, A. E. *Critical Stability Constants*, Vol.s 1 and 4: Inorganic Complexes; Plenum Press: New York, 1976. (b) Cernochova, K.; Mathur, J. N.; Choppin, G. R. *Radiochim. Acta* **2005**, *93*, 733−739. (c) Smith, T. D. *J. Inorg. Nucl. Chem.* **1959**, *11*, 314−319.

(8) Mathur, J. N.; Thakur, P.; Dodge, C. J.; Francis, A. J.; Choppin, G. R. *Inorg. Chem.* **2006**, *45*, 8026−8035.

(9) Runde, W. *Los Alamos Science* **2006**, *26*, 392−411.

(10) Vercouter, T.; Vitorge, P.; Trigoulet, N.; Giffaut, E.; Moulin, C. *New J. Chem.* **2005**, *29*, 544−553.

(11) Vercouter, T.; Vitorge, P.; Amekraz, B.; Giffaut, E.; Hubert, S.; Moulin, C. *Inorg. Chem.* **2005**, *44*, 5833−5843.

(12) Verma, S.; Saxena, M. C. *Proc. Indian Acad. Sci.* **1987**, *99*, 217−222.

(13) Thakur, P.; Pathak, P. N.; Gedris, T.; Choppin, G. R. *J. Solution Chem.* **2009**, *38*, 265−287.

(14) Mathur, J. N.; Cernochova, K.; Choppin, G. R. *Inorg. Chim. Acta* **2007**, *360*, 1785−1791.

(15) Choppin, G. R.; Thakur, P.; Mathur, J. N. *Coord. Chem. Rev.* **2006**, *250*, 936−947.

(16) Boukhalfa, H.; Reilly, S. D.; Smith, W. H.; Neu, M. P. *Inorg. Chem.* **2004**, *43*, 5816−5823.

(17) Dumonceau, J.; Bigot, S.; Treuil, M.; Faucherre, J.; Fromage, F. *Rev. Chim. Minér.* **1980**, *17*, 58−64.

(18) Barkleit, A.; Geipel, G.; Acker, M.; Taut, S.; Bernhard, G. *Spectrochim. Acta. A* **2011**, *78*, 549−552.

(19) Thakur, P.; Conca, J. L.; Van de Burgt, L. J.; Choppin, G. R. *J. Coord. Chem.* **2009**, *62*, 3719−3737.

(20) Thakur, P.; Pathak, P. N.; Gedis, T.; Choppin, G. R. *J. Solution Chem.* **2009**, *38*, 265−287.

(21) Natrajan, L. S. *Coordin. Chem. Rev.* **2012**, *256*, 1583−1603.

(22) Faulkner, S.; Pope, S. J. A.; Burton-Pye, B. P. *Appl. Spectrosc. Rev.* **2005**, *40*, 1−31.

(23) Morgenstern, M.; Klenze, R.; Kim, J. I. *Radiochim. Acta* **2000**, *88*, 7−16.

(24) Kimura, T.; Nagaishi, R.; Kato, Y.; Yoshida, Z. *Radiochim. Acta.* **2001**, *89*, 125−130.

(25) Clark, D. L.; Hobart, D. E.; Neu, M. P. *Chem. Rev.* **1995**, *95*, 25−48.

(26) Carnall, W. T.; Fields, P. R. *J. Am. Chem. Soc.* **1959**, *81*, 4445−4449.

(27) Gans, P.; Sabatini, A.; Vacca, A. *Talanta* **1996**, *43*, 1739−1753.

(28) Yusov, A. B. *J. Radioanal. Nucl. Ch.* **1990**, *143*, 287−294.

(29) Beitz, J. V. *J. Alloys Compd.* **1994**, *207/208*, 41−50.

(30) Kimura, T.; Kato, Y. *J. Alloys Compd.* **1998**, *271*−*273*, 867−871.

(31) Runde, W. H.; Schulz, W. W. *The Chemistry of the Actinide and Trans-actinide Elements: Chapter 8*; Springer: The Netherlands, 2010.

(32) Matonic, J. H.; Scott, B. L.; Neu, M. P. *Inorg. Chem.* **2001**, *40*, 2638−2639.

(33) Van der Lee, J. A. Users Guide to CHESS, Another Speciation and Surface Complexation Computer Code, École des Mi1nes de Paris, Fontainebleau, 1998.